Journal of Applied Polymer Science

Vinculin focal adhesion of osteoblast-like cells on PEEK coated with ultra-thin polymer nano films

Firas Awaja,[1] Eleonora Carletti,[2] Walter Bonani,[2] Giorgio Speranza[1]

[1]Center for Materials and Microsystems, PAM-SE, Fondazione Bruno Kessler, Via Sommarive 18, Trento, Italy

[2]Department of Industrial Engineering, BIOtech Research Center and INSTM Research Unit, University of Trento, Via Sommarive 9, Trento, Italy

Correspondence to: F. Awaja (E-mail: awaja@fbk.eu)

ABSTRACT: PEEK is the polymer of choice to replace metal encapsulants and other parts in active medical implants fixated into bone. The current challenge is to improve its biocompatibility with bone tissue to ultimately achieve osseointegration. PEEK sheets surfaces coated with plasma deposited nano thin polymer films using CH_4, ($CH_4 + O_2$) and ($CH_4 + N_2$) gases. PEEK samples plasma treated with nonpolymerizing gases (O_2) were also used for comparison. The adhesion performance of osteoblast like cells on the plasma-treated PEEK surfaces and the presence of Vinculin in these cells were evaluated after long culturing period (12 days). X-ray photo-electron spectroscopy and Auger spectroscopy were used to provide surface molecular information, surface hardness and molecular density. All plasma-treated surfaces retained functionality after the sterilization process. PEEK surfaces with high number of oxygen functional groups and particularly oxygen rich thin polymer coating (plasma deposition using CH_4+O_2 gas mixture) resulted in strong cellular adhesion strength and large Vinculin amount. Further, osteoblast-like cells responded better to surfaces with lower molecular density acting like another signal for cell adhesion. The osteoblast-like cells response was weaker for surfaces with both thin films with nitrogen functional groups and nonfunctional (nonpolar) films. Furthermore, thin films rich in nitrogen functional groups repelled the cells, showed abnormal cells shape, smaller Vinculin amount and induced thicker cellular clusters with poor spread. © 2015 Wiley Periodicals, Inc. J. Appl. Polym. Sci. **2015**, *132*, 42181.

KEYWORDS: biomaterials; proteins; surfaces and interfaces

Received 24 November 2014; accepted 1 March 2015

DOI: 10.1002/app.42181

INTRODUCTION

Active medical implants such as the Cochlear Implant, Deep Brain Stimulator (DBS) and the Bionic Eye (BEYE) are devices used to restore lost sensory function or functionality of a human organ. They are designed to be implanted in the human body and function for many decades without complications. Major weaknesses with the metal made devices are detachment,[1] leakage,[1] debris contamination,[2] and tissue loosening around the device.[2–5] These complications are often corrected through repeated surgeries.

Techniques that enables medical implants to be made entirely from polymers have been investigated recently[6–13] and have the potential to resolve most of the problems associated with metal made implants. Earlier reports were focusing largely on providing materials solutions that enables hermetic bonding, an essential step for implants encapsulation. The following technical steps would include providing the implants with enhanced biocompatibility (cell adhesion and metabolism), stability and immovability through osteo integration. Osseointegration also prevents infection and body rejection. Further, it will simplify implant procedures especially for DBS implant.

Cell adhesion to polymer surfaces depends on multiple factors including surface hydrophilicity, morphology (such as crystalline and amorphous domains), topography (roughness), surface energy, surface charge, and chemical composition.[13,14] PEEK exhibits a hydrophobic bio-inert surface characteristic which is not favorable for protein absorption and cell adhesion.[15,16] Therefore, for tissue integration the surface of PEEK needs to be modified to enhance the ability for cells to attach.

Plasma-assisted chemical vapour deposition (PACVD) is the process of choice for depositing functional polymer thin films through controlling the bombarding ions energy and type and the plasma deposition time. The deposition mechanism include the process of elastic collisions of precursor ions with the nuclei of the substrate material in a process called ion subplantation. The result of ion supplantation is either displacement of surface

atom (high energy collision) or an ion that will stick to the surface (low energy ions). In theory, the processes of displacement and deposition is controlled via manipulating the bombardment energy and the precursor ions. Controlling the plasma bombardment energy define the percentage of the sp3 bonding state, which gives rise to the diamond-like properties in plasma deposited thin films. Lower bombardment energies creates polymer-like films that are soft and shown to have the elasticity range that encourages cells adhesion and survival.[6]

The MG63 osteoblast-like osteosarcoma cell line was chosen for this study as it exhibits many osteoblastic characteristics such as the ability to synthesize osteocalcin and collagen I. Therefore, MG 63 cells can serve as a model cell line to study the interaction of bone cells with implant materials.[2,17–21] Vinculin is a cellular protein that plays a vital role in providing strong attachment between the cell and its environment.[22–25] Its presence indicates the evolution of small dot-like adhesion sites into a strong streak-shaped focal adhesion point.[25] Despite the confirmed association between the presence of Vinculin and cellular adhesion, little is known about the adhesion chemistry or the mechanism of adhesion.

Previous investigations on cellular adhesion to plasma-treated polymer surfaces[6–9,26–28] identified favourable plasma condition factors such as polymerizing gas ratio, forward power, and plasma time for the surface preparation of PEEK for medical implants. A mixture of oxygen and methane (1 : 1 ratio) produced a functionalized thin film coating that improved PEEK adhesion to cells up to 85%.[6] However, these earlier studies were mostly qualitative, conducted for relatively short time and no evaluation of the presence of adhesion-related proteins were shown.

In this study, we conduct a longer (12 days) cell study, pass the initial cellular migration, and spreading process, using osteoblast cell line with stabilised and functionalised ultra-thin polymer film and compare it to other surface preparation treatments of PEEK. We also seek to produce more accurate and quantitative adhesion and growth information by evaluating the presence and functionality of specific protein Vinculin which is associated with cells adhesion. Furthermore, by using XPS and Auger spectroscopy, we aim to provide molecular information regarding surface chemistry, hardness, and molecular density as another signal for cellular growth.

EXPERIMENTAL

Materials

Semi-crystalline PEEK as a 500 μm thick film (APTIV 1000, Victrex plc, UK) was used in this study. PEEK has 32% crystallinity, with glass transition and melting temperatures of 147.3°C and 345.3°C respectively, as measured by temperature modulated differential scanning calorimetry.

Plasma Deposition

The plasma activation equipment used in this study were made in house as shown in Figure 1. The PECVD plasma reactor consisted of a vacuum chamber maintained at 10^{-8} mbar range during nonworking conditions to avoid contamination. Sample insertion in the reactor is performed through a load-lock

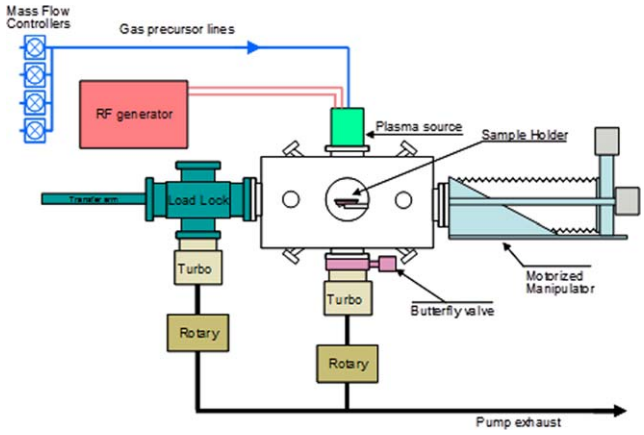

Figure 1. Schematics of the plasma reactor setup. [Color figure can be viewed in the online issue, which is available at wileyonlinelibrary.com.]

avoiding system venting. The plasma source is a Copra GTE200 source which generates an intense plasma density through a cyclotronic resonant magnetic field. The applied power was 200 W which allowed efficient film deposition without damaging the PEEK samples used as a substrate. During the deposition process the pressure inside the reactor was maintained constant at 0.15 mbar by adjusting a butterfly valve. Flow rate of inlet gases were kept at 40 sccm, mixture of 2 gases kept at 1 : 1 rato (20+20 sccm). Other variables were kept constant such as magnet current at 2 amp, magnet voltage at 6.2 v. Plasma treatment time was kept at 15 min for all experimental runs. Amount of inlet gas(es) delivered to the plasma reactor were controlled using mass flow controllers (MKS Instruments MA-USA).

For this study, four samples were selected with different plasma precursor gas ratio in addition to the untreated control. PEEK samples were plasma treated using O_2, CH_4 gasses alone and then a mixtures of CH_4+O_2 and CH_4+N_2 were also used. The CH_4+O_2 samples was produced using three different experimental runs and was measured and analyzed accordingly including the biological cell studies for reproducibility and repeatability evaluation.

XPS

X-ray photoelectron spectra were acquired for different PEEK-treated samples. The analyzer is a Kratos Axis DLD Ultra operated in spectral mode. The pass energy was 160eV for the acquisition of 1250-0 eV wide scans while it was reduced to 40 eV in the case of the acquisition of high resolution core-line spectra. Since the substrate is a nonconducting polymer, charge compensation was utilized. The instrument is equipped with a flooding electron gun which is coaxial to the analyzer axis making the compensation particularly efficient. Compensation conditions were set in order to maximize peak intensity and reduce the full-width at half maximum (FWHM). The average resolution of the instrument in this experimental condition was ~0.35 eV. Core line analysis was performed with a homemade software based on the R platform (The R Project for Statistical Computing, http://www.r-project.org/). Linear background subtraction was utilized and Gaussian component was used to perform the peak fitting. Quantification was carried out utilizing the sensitivity factors provided by the instrument manufacturer.

Table I. Shows the Elements Relative Concentrations of the Plasma-Treated PEEK Samples as Measured by XPS

Sample	N_2%	N_2(S)%	O_2%	O_2(S)%	C %	C(S)%	O/C (%)	O/C (%) (S)
Untreated	0	0	13.1	12.0	86.9	88.1	15.1	13.6
Plasma O_2	0	0	23.4	15.9	76.6	84.1	30.6	20.7
Plasma CH_4+N_2	16.5	12.4	3.7	9.8	79.9	77.8	4.6	12.5
Plasma CH_4	0	0	3.3	6.4	96.7	93.6	3.4	6.8
Plasma CH_4+O_2	0	0	20.7	16.5	79.3	83.5	26.1	19.7

S, sterlized; standard deviation (CH_4+O_2 sample) = 0.3%.

Auger Spectroscopy

Auger spectra were acquired with a pass energy of 40 eV for an attempt to classify the deposited films hardness and molecular density. This generally performed by estimating the Auger width δ which form the first derivative of the Auger spectrum. This requires the integral spectrum to be filtered to remove the main part of noise which would affect the first derivative preventing the recognition of its maximum and minimum positions. A digital Butterwort filter with 1 dB amplification in the pass band and −50 dB rejection in the stop band was designed to attain the above mentioned objective. Cut-off frequency of the pass-band corresponds to oscillations having period equal to 100 spectral points (i.e., 5 eV). The Auger width was calculated by fitting the Auger feature with four Gaussian components to determine the feature width Δ as described in our previous work.[29] The analysis of the Auger spectra were performed only on nonsanitized samples to avoid introduction of higher level of complexity and interpretation errors.

In Vitro Cell Culture

Plasma-treated PEEK samples (5 × 5 mm^2), were sterilized using autoclave (120°C at 1 bar for 45 min). Then, the plasma-treated PEEK samples were seeded by a suspension of human osteosarcoma derived osteoblasts (MG63) using a minimum essential medium (MEM) supplemented with 10% fetal bovine serum (FBS), 1% penicillin, 1% vitamin, and 1% nonessential amino acids.

All plasma-treated PEEK samples, after seeding, were incubated at 37°C in a 5% CO2 atmosphere incubator, with medium changes every 2−3 days. Two different in vitro tests were performed. In the first test, samples were seeded using a cell concentration of 10^4 cells/sample (confined drop method with a 20 μL of cell suspension). Cell culture was performed under static conditions using 48-well plate. Cell proliferation over 12 days of culture (three time points were analyzed, 1, 5, 12 days) was measured by PicoGreen assay (Quant-iT Pico Green dsDNA Assay Kit, Life Technologies; Carlsbad, CA 92008) and visualized by confocal laser microscopy (CLM) (Nikon Eclipse; Ti-E) after staining with Oregon Green (Life Technologies; Carlsbad, CA) and DAPI (Sigma-Aldrich; St. Gallen, Switzerland) staining.

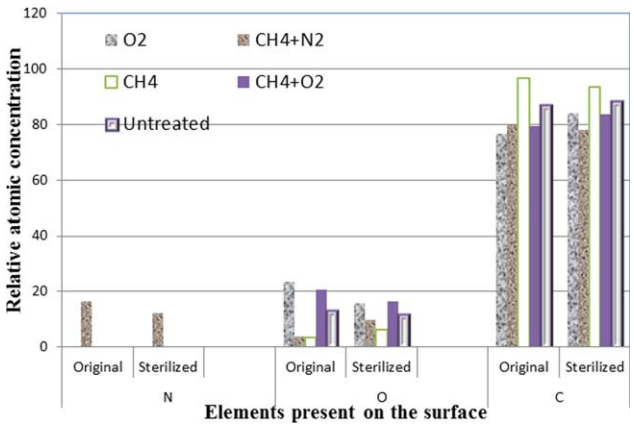

Figure 2. shows the difference in surface relative atomic concentration before and after sanitization. [Color figure can be viewed in the online issue, which is available at wileyonlinelibrary.com.]

In a second test, a deeper focus on cell attachment was investigated involving the use of a specific staining for the cytoskeletal adhesion protein Vinculin (Life Tecnologies; Carlsbad, CA). Cell culture was modified, 10^5 cells suspended in 500 μL of medium were seeded on samples placed in a 48-well plate. After 24 h from seeding, samples were fixed by a 4% formaldehyde solution and stained as explained below.

For DNA quantification a total 5 PEEK samples were analysed for each experimental group. Confocal analysis was performed on triplicates.

Cell Proliferation

DNA quantification was used to measure the number of cells per sample during the culturing time, using the PicoGreen assay. At fixed time periods, the medium was removed from wells and the samples were washed with phosphate-buffered saline (PBS). Totally, 500 μL of 0.05% Triton X was used to completely cover the samples before freezing and storing at −20°C until analysis. After thawing each sample was sonicated for 10 s using an ultrasonic processor (UP400S Hielscher, Ultrasonics GmbH; Teltow, Germany) equipped with a 7 mm sonotrode tip. Then, 100 μL of the PicoGreen working solution was

Table II. Shows the Relative Atomic Concentration of the Functional Groups on the Surface of the Plasma Treated for C1s as Measured by XPS, St. Deviation for C—O for the CH_4+O_2 Sample = 0.2%

Sample	C—C/H	C—O	C=O	O—C=O	C—NH
Untreated	65.9	15.7	3.6	0	0
Plasma O_2	51.0	16.5	6.6	2.6	0
Plasma CH_4+N_2	51.7	7.1	2.6	0.6	16.5
Plasma CH_4	88.0	5.9	2.0	0.8	0
Plasma CH_4+O_2	53.2	22.0	3.0	1.4	0

Table III. Shows the Relative Atomic Concentration of the Functional Groups on the Surface of the Plasma Treated for O1s as Measued by XPS. St. Deviation (for C—O for the CH_4+O_2 sample = 0.2%)

Sample	C=O	C—O	C—O Ar	H_2O
Untreated	3.1	2.1	7.4	0.5
Plasma O_2	6.1	1.5	13.8	2.1
Plasma CH_4+N_2	3.4	0.0	0.14	0.1
Plasma CH_4	2.9	0	0.3	0.0
Plasma CH_4+O_2	7.2	0	12.9	0.7

added to 100 μl of the cell lysate in a 96-well plate; each sample was measured in triplicate. Fluorescence output was read by a spectrophotometer (excitation wavelength: 485 nm, emission wavelength: 538 nm; Tecan Infinite M200 Pro; Mannerdorf, Switzerland). To correlate fluorescence to DNA concentration, a calibration curve was produced using DNA standards at known concentrations, provided with the assay. The DNA amount of each sample was divided by 7.7 pg of DNA, the average amount of DNA in a human cell according to the literature,[30] to finally obtain the number of cells per sample.

Cell Morphology and Distribution, Oregon Green, and DAPI Staining

Cell morphology and distribution were visualized by Oregon Green 488 Phalloidin and 4'6-diamidino-2-phenylindole (DAPI) stainings. Oregon Green 488 Phalloidin stains actin filaments of cytoskeleton resulting in green fluorescence while DAPI stains nuclei resulting in blue fluorescence. Cells were fixed with a 4% formaldehyde in PBS, permeabilized with Triton X (0.2% Triton X in PBS) and stained with Oregon Green 488 and DAPI, according to the manufacturer's protocol. After three rinses with PBS, samples were examined by CLM.

Vinculin Expression

To detect the cytoskeletal protein Vinculin, involved in cell adhesion and migration, cells were labeled with a primary rabbit antibody to human Vinculin. Alexa Fluor 546 goat anti-rabbit (Life Tecnologies; Carlsbad, CA) was used as secondary antibody, resulting in a red color. Briefly, cells were fixed with 4% formaldehyde in PBS and permeabilized with 0.2% Triton X in PBS; after three rinses with PBS, the samples were incubated with the primary antibody (in PBS containing 1% bovine serum albumin (BSA)) for 1.5 h at room temperature. The seeded PEEK samples were then rinsed with 1% BSA solution in PBS and incubated with Alexa Fluor 546 goat anti-rabbit secondary antibody for 1.5 h at room temperature. Cells were then stained with Oregon Green 488 Phalloidin and DAPI, as described above. After three rinses with PBS, samples were analyzed by CLM. Confocal images were analyzed with ImageJ software (National Institutes of Health, Bethesda, MD) performing a semiquantitative comparison between the samples in terms of Vinculin density. A value of Vinculin spots per cell was obtained by dividing the number of Vinculin spots detected in a single confocal image by the number of nuclei per picture. For comparison, results were normalized with respect to the Untreated PEEK sample. The value of Vinculin area per cell is based on the fractional area of each image that is covered by Vinculin spots divided by the number of nuclei per picture.

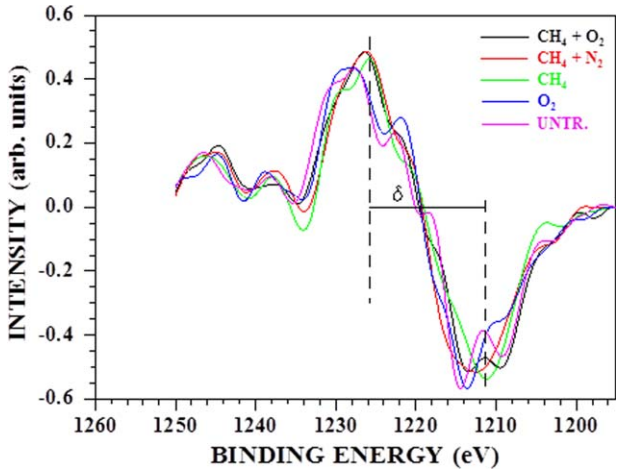

Figure 3. First derivative of the filtered Auger spectra. The oscillations of the first derivative in the minimum region (red line) renders the estimation of the width δ rather complex. [Color figure can be viewed in the online issue, which is available at wileyonlinelibrary.com.]

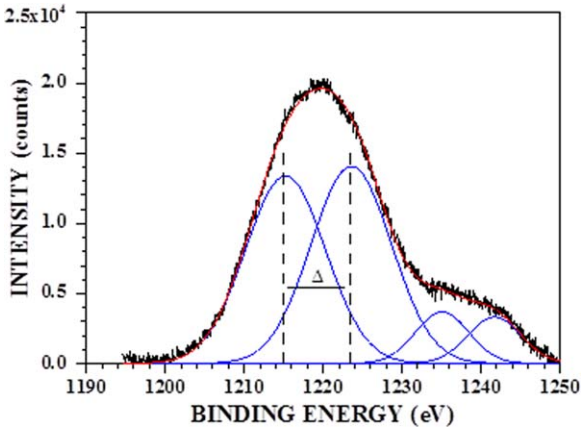

Figure 4. First derivative of the filtered Auger spectra. The oscillations of the first derivative in the minimum region (red circle) renders the estimation of the width δ rather complex. [Color figure can be viewed in the online issue, which is available at wileyonlinelibrary.com.]

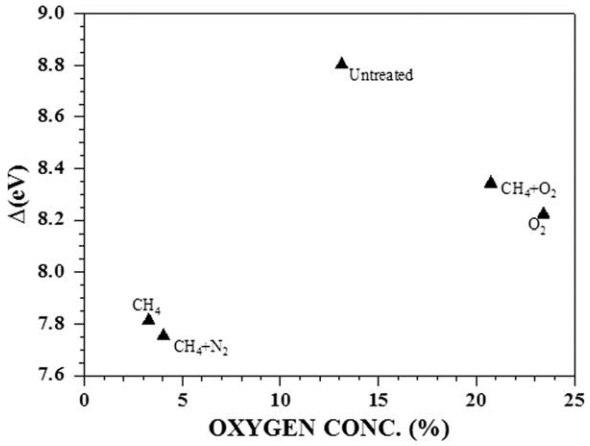

Figure 5. Trend of the width Δ as a function of the oxygen concentration.

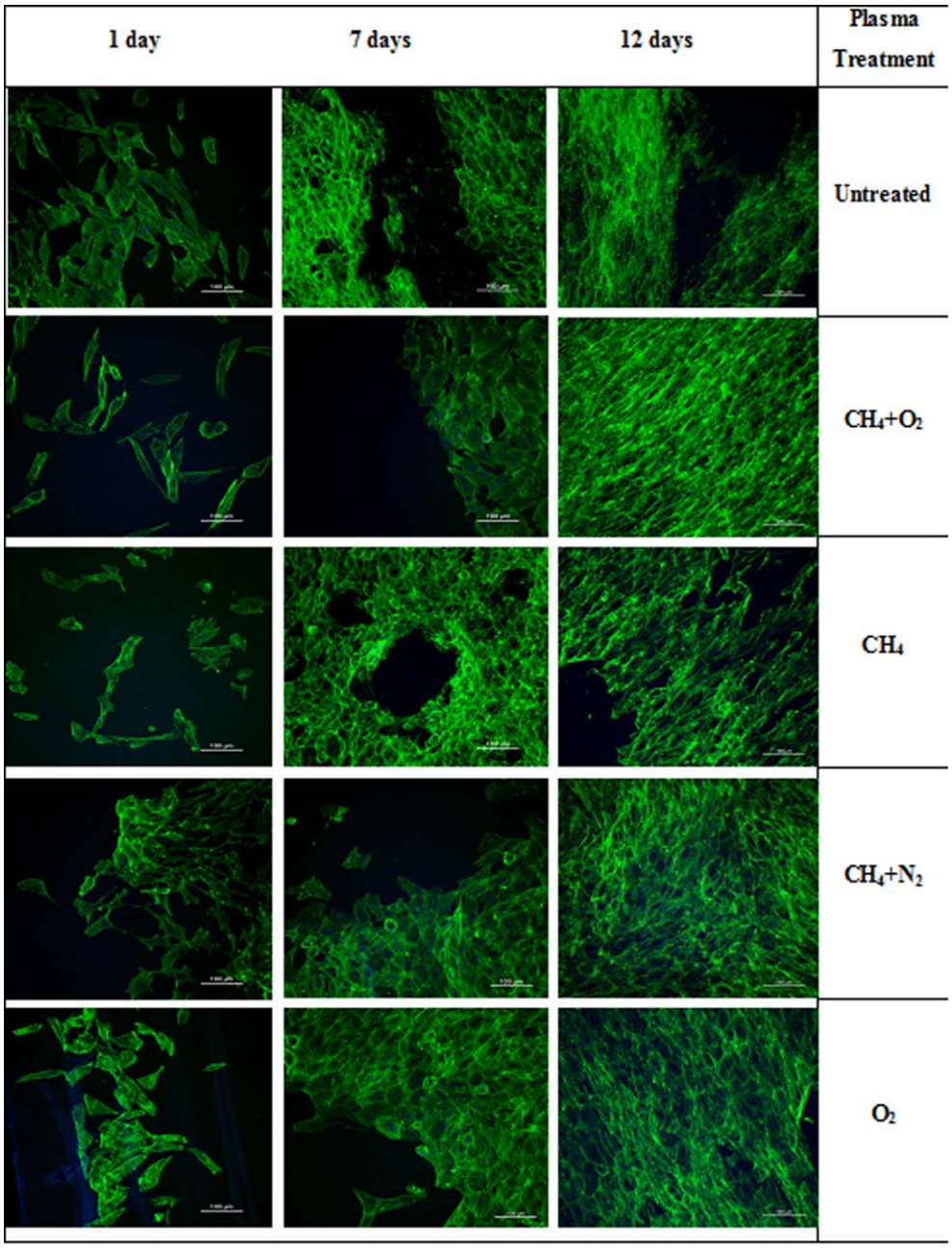

Figure 6. Representative confocal microscopy images of untreated and treated PEEK samples seeded with MG63 labeled with Oregon Green 488 Phalloidin (cytoskeleton, green), DAPI (nuclei, blue) at different culture. [Color figure can be viewed in the online issue, which is available at wileyonlinelibrary.com.]

RESULTS AND DISCUSSIONS

XPS Results

Table Ishows the XPS analysis results of the plasma-treated PEEK samples. The table also shows the relative concentration of N, O, and C before and after the treated PEEK samples sterlization process. PEEK samples that are treated with oxygen, either alone or with CH_4, showed almost double the amount of oxygen on the surface compared with the untreated sample. The CH_4-treated samples (either alone or with N_2) showed a lower oxygen content on the surface when compared with the untreated sample. The later might indicates a thin film surface coating that masked some of the oxygen atoms that are present natively in PEEK strucutre. The oxygen concentration on the surface of the CH_4-treated PEEK sample is probably a result of the surface reactions with oxygen that is present in the surrounding environment after the plasma treatment.

The relative atomic concentration of PEEK-treated samples were also measured using XPS after the sterlization process. Different samples exhibited different behavior after sterilization; however, the effect on functionality is deemed to be moderate (as derived from Table I and also shown in Figure 2). Samples treated with CH_4 and CH_4+N_2 showed an increase (almost doubled) in

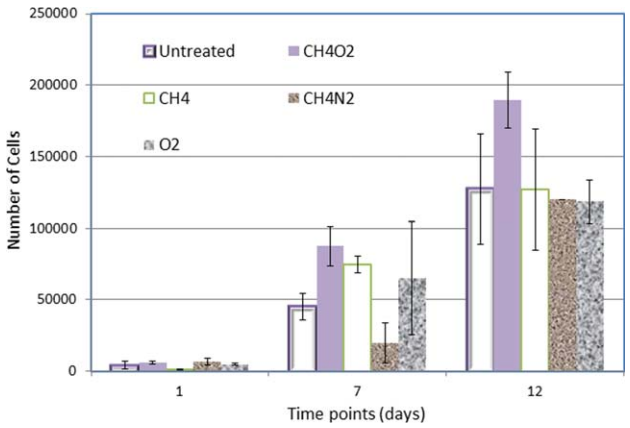

Figure 7. Number of samples as a function of culture days for all treated and untreated samples. [Color figure can be viewed in the online issue, which is available at wileyonlinelibrary.com.]

oxygen relative concentration after sterilization due to the exposure to higher temperature. Nitrogen functionality slightly decreased in the case of PEEK samples plasma treated using CH_4+N_2 mixture. Sterilization had no noticeable effect on the untreated sample while samples plasma treated with O_2 and CH_4+O_2 showed a moderate reduction in oxygen concentration (32% and 20%, respectively) as a result of sterilization. All samples, however, retained most of the surface chemistry attributes after sanitization.

Tables II and III show the relative atomic concentration of the functional groups on the surface of the plasma-treated samples for C1s and O1s regions. The samples that are treated with CH_4+O_2 and O_2 along with the untreated sample showed higher C—O functional groups than other samples. Plasma treatment using O_2 only generated double as much C═O functional groups than CH_4+O_2 sample and triple as much other plasma-treated samples.

Auger Analysis

Auger analysis was conducted on the plasma-treated PEEK samples to provide some insight regarding sp3 hybridization, and in turn the thin film hardness and molecular density as a function of cellular response. There are few methods to determine the width of the Auger feature of a given chemical element. The most common method utilizes the derivative of the Auger spectrum KVV spectra and computes the distance between the main positive and negative peaks. Despite the high quality of the obtained first derivative spectra, it is rather complex to manipulate due to the presence of spectral features that introduce oscillations which makes interpretation complex (see Figure 3). The Auger spectrum was fitted with four Gaussian components as shown in Figure 4 to calculate the width Δ. If quality of the spectra is acceptable, as in our case, this procedure is noise independent and the parameter Δ correctly reflects the spectral width.

Figure 4 example of estimation of the Auger width Δ utilizing the four Gaussian method.

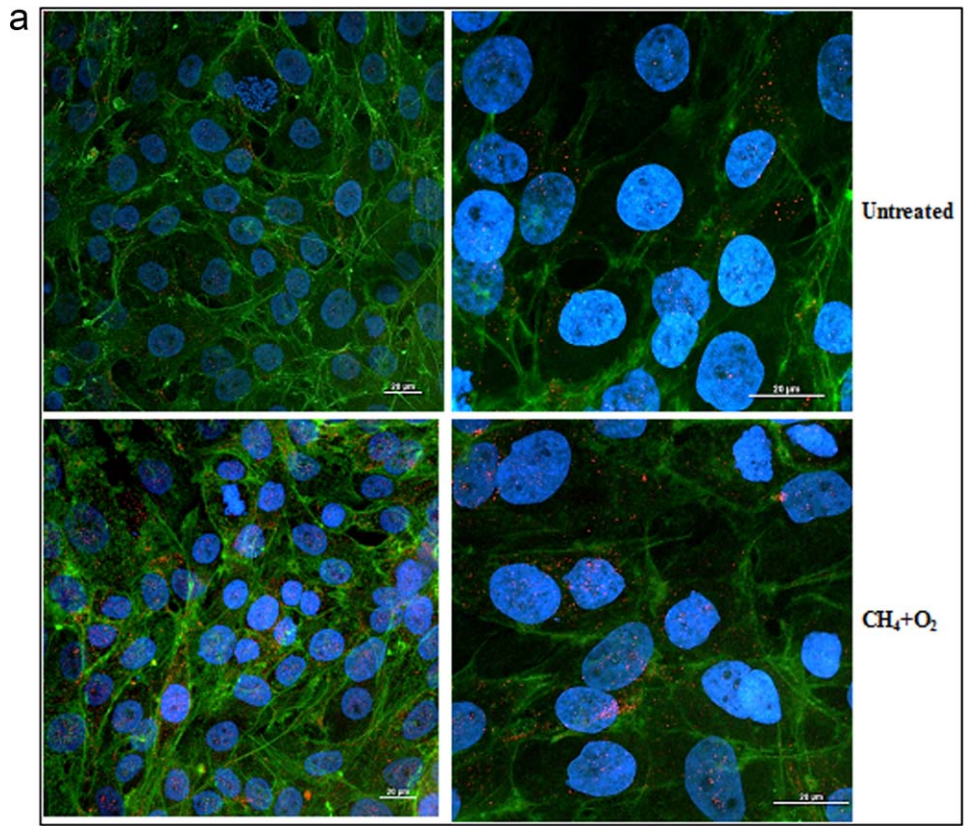

Figure 8. Representative confocal images of MG63 cells stained with Oregon Green 488 Phalloidin (cytoskeleton, green), DAPI (nuclei, blue) and rabbit anti-Vinculin (focal adhesion, red) seeded on different plasma treated PEEK surfaces. (scale bar 20 μm). [Color figure can be viewed in the online issue, which is available at wileyonlinelibrary.com.]

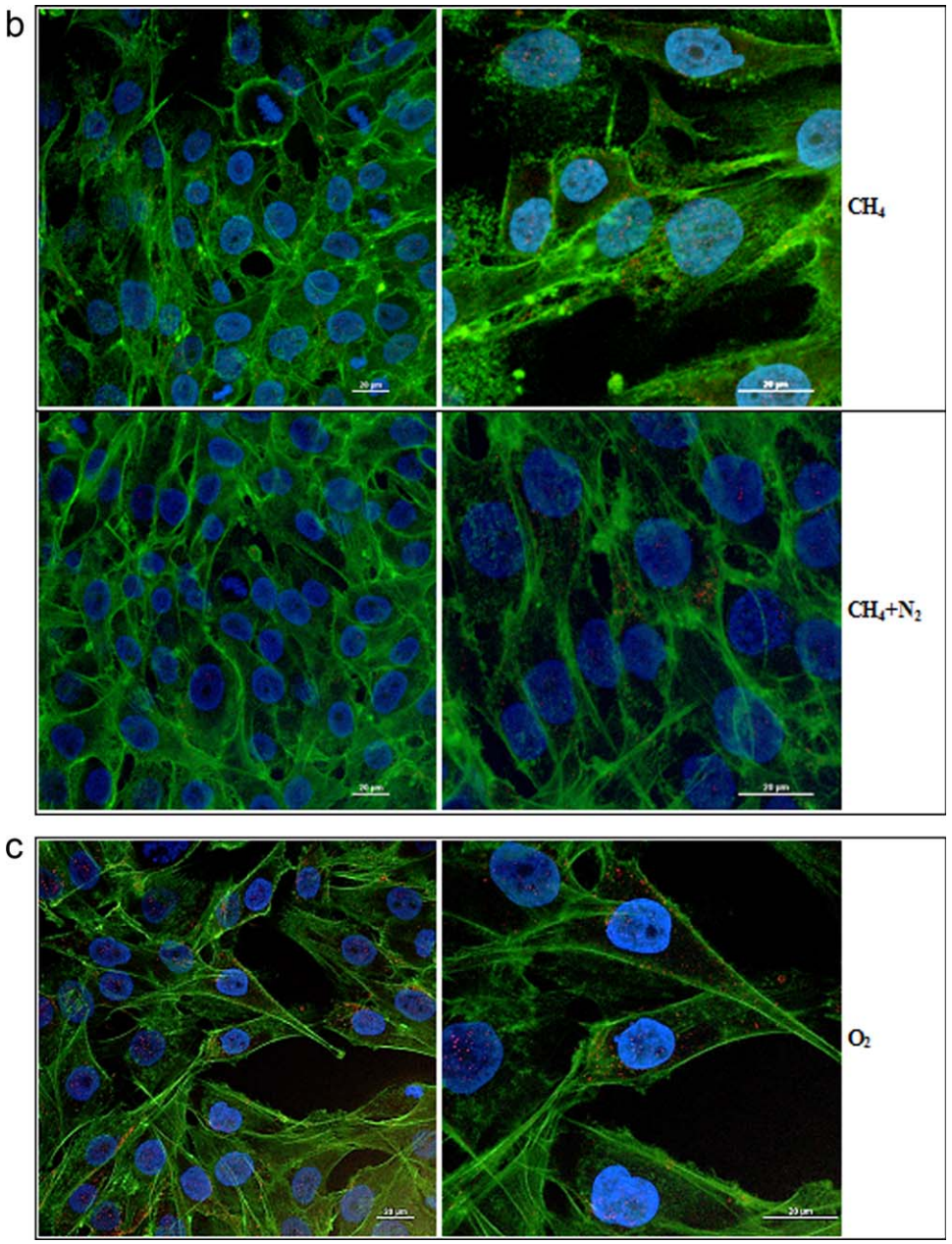

Figure 8. (Continued)

The Auger feature is modulated by the surface chemistry and structure of the analyzed material.[31–33] The results of the analysis performed on the Auger spectra are reported in Figure 5.

Figure 5 shows the width Δ as a function of the oxygen concentration found on the substrate surface. The Auger analysis clearly distinguish between the untreated sample and those with high oxygen ($CH_4 + O_2$ and O_2 plasma-treated PEEK) and low oxygen content (CH_4 and $CH_4 + N_2$ plasma-treated PEEK). In the case of carbon based materials, smaller width is associated with higher hardness of the material as a result of higher density of sp3 hybridized carbon atoms. All plasma-treated samples exhibited harder surfaces than the untreated PEEK sample. Samples treated with O_2 and $CH_4 + O_2$ showed softer surfaces with less dense molecular structure than samples that are plasma treatment without the presence of oxygen.

Cell Culture Evaluation

Cell cultures were performed in order to evaluate cellular responses to functionalized ultra-thin films deposited on PEEK surfaces. The project objectives include cellular growth, adhesion, spreading, morphology, and potential for osseointegration. A separate cell culture study was devised to particularly inspect the adhesion and spreading through the evaluation of the cytoskeletal protein Vinculin concentration as a function of the different thin film arrangements.

In the first *in vitro* test, proliferation over 12 days of static culture was evaluated by PicoGreen analysis. Furthermore, confocal laser microscopy was used to visually demonstrate cell behavior, morphology and arrangement on the substrates. Well adherent cells were observed on all PEEK samples within 24 h of seeding (representative confocal images reported in Figure 6).

As far as cells distribution on the samples after 24 h, we observed that a consistent amount of cells occupied the edge/border of the samples, while the inner area was scattered with isolated colonies of cells. This is consistent with previous observations in the literature, cells usually prefer the ragged, irregular surface on the edge, while a relatively smooth surface is not the most favorable substrate for cell attachment.

Initially the cells showed strong response to the surface chemistry. There were differences in the appearance of those isolated clusters of cells. PEEK samples plasma treated with CH_4O_2 and CH_4 had more developed, low-density islands and cells were distributed homogeneously. On the other hand, PEEK samples plasma treated with $CH_4 + N_2$ showed closely packed cell clusters were cells tended to adhere to each other rather than to the surface, indicating a lower cell-substrate compatibility. Samples plasma treated with O_2 had a mixed behavior. This response could be related to surface molecular density or hardness since O_2 plasma-treated samples showed lower compactness than the samples treated with CH_4 only.

After 7 days, cells reached a high degree of surface coverage, where large portions of the surface were covered with a dense, homogeneous carpet of cells. Confocal images were taken at boundary between cell carpet and empty regions. Cell proliferation is high for each sample. In the case of the untreated PEEK cells appeared to grow in multilayers rather than colonize the free surface. On the contrary, cells appeared to be more homogeneously distributed on CH_4+O_2, O_2, and N_2 samples, where empty areas were clearly more limited. It's worth noting that the clustering effect is more evident when cells are few, that is at shorter time points (1 day in our case). After 7 days cells are obviously increased in number and clusters cannot be appreciated anymore, cells cover more evenly on the surface. Most likely the small clusters develop into larger areas and eventually they merge together. This is also can be regarded as a measure for the materials biocompatibility. If the substrate is not biocompatible, cells do not even attach. It is unclear at this stage, if the cells on CH_4+N_2 plasma-treated samples and cells on the other samples are in the same conditions. This ambiguity led to the second study which will be discussed at a later stage in this article.

The number of cells on the samples at the three time points was determined from total DNA content and shown in Figure 7. All samples showed a significant cell proliferation as times progresses indicating healthy cells growth. However, PEEK samples that are plasma treated with CH_4+O_2 showed significantly higher proliferation when compared with all other samples. Cells shape were elongated and spread on all plasma-treated surfaces after the first day or cell culture. After 7 days, however, images of cells on the plasma-treated samples of CH_4 and CH_4+N_2 (Figure 7) showed some circular shaped cells indicating poor adhesion. The trend remained for these two samples pass 12 days of incubation despite the relative increase of cell numbers.

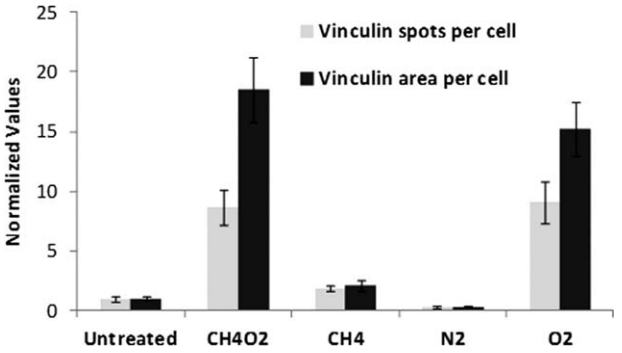

Figure 9. shows a semi-quantitative assessment of Vinculin spots and area per cell for treated and untreated PEEK samples. Presented values were normalized with respect to the untreated PEEK.

After the conclusion of the first 12 days study, it was obvious that more information is needed. In particular, cell morphology and adhesion. Vinculin is a cell protein involved in integrin-mediated cell–matrix adhesions and cadherin-mediated cell–cell junctions. Vinculin-actin binding is necessary for mechanically resilient focal adhesions and to strengthen the focal adhesion. Vinculin controls the transmission of intracellular and extracellular mechanical cues that are important for the spatiotemporal assembly, disassembly, and reorganization of focal adhesions to coordinate polarized cell motility.

After 24 h of cell culture (Figure 8), all the surfaces demonstrated to host cells, able to spread and adhere over the surfaces. However, PEEK samples that are plasma treated with CH_4+O_2 (in particular) and O_2 showed a higher quantity of Vinculin protein, resulting in more evident red spots. Conversely, cells seeded on the untreated PEEK showed limited amount of Vinculin and lower than the PEEK samples treated with CH_4 and N_2. Accordingly, even if cells appear spread and homogeneously distributed on all the samples, a deeper analyses demonstrates a higher attitude for the cells seeded on the oxygen rich surfaces to express the Vinculin protein. This could mean that even if cells appear spread, their adhesion or their ability to migrate can be different from other cells similarly spread.

The confocal images were further analyzed by the image processing program Image J to quantify the Vinculin signal. Two measures were performed: vinculin spots per cell and vinculin area per cell Figure 9 shows higher normalized value for PEEK samples treated with CH_4+O_2 and O_2 that have higher polarity and oxygen relative concentration. Sample that is treated with CH_4 and Nitrogen showed the least values which indicate a tendency for these cells to respond to oxygen functionalities and not nitrogen and nonpolar functionalities.

CONCLUSIONS

The polymer thin films survived different regimes of sterilization and it retains most of its functionality and performance. This is largely due to the strong covalent bonding that connect them to

the polymer surface and to the dense cross-link structure that provide limited reactivity including hydrolysis reactions. All plasma treatments improved PEEK biocompatibility significantly. Vinculin, a protein linked to focal adhesion, was clearly present in samples with greater oxygen functionality. Samples treated with CH_4+O_2 showed strong promise regarding future work towards the osteo integration of PEEK. Samples treated with CH_4+N_2 showed undesired cellular clustering and abnormal cellular behaviour. Plasma treatment using CH_4+N_2 is a candidate process for coating devices in which cellular growth/bio films are not desired.

ACKNOWLEDGMENTS

The first author would like to acknowledge the financial support from the European Union under the FP7 COFUND Marie Curie Action.

REFERENCES

1. Jain, R.; Mukherji, S. K. *Clin. Radiol.* **2003**, *58*, 4, 288.
2. Kotzar, G.; Freas, M.; Abel, P.; Fleischman, A; Roy, S.; Zorman, C.; Moran, J. M.; Melzak, J. *Biomaterials* **2002**, *23*, 2737.
3. Lin, T. W.; Corvelli, A. A.; Frondoza, C. G; Roberts, J. C.; Hungerford, D. S. *J. Biomed. Mater. Res.* **1997**, *36*, 137.
4. Kurtz, S. M.; Devine, J. N. *Biomaterials* **2007**, *28*, 4845.
5. Sereno, N. *Eur. Med. Device Tech.* **2010**, *1*, 22.
6. Awaja, F.; Bax, D. V.; Zhang, S.; James, N.; McKenzie, D. R. *Plasma Processes Polym.* **2012**, *9*, 355.
7. Awaja, F.; Zhang, S.; James, N.; McKenzie, D. R. *Plasma Proc. Polym.* **2012**, *9*, 174.
8. Awaja, F.; McKenzie, D. R.; Zhang, S.; James, N. *Appl. Phys. Lett.* **2011**, *98*, 211504.
9. McKenzie, D. R.; James, N. L.; Grace, J. R.; Amanat, N.; Awaja, F.; Chaminade, C. L. E. US Patent App. 13/036,843.
10. Zhang, S.; Awaja, F.; James, N.; McKenzie, D. R.; Ruys, A. J. *Colloids Surf. A* **2011**, *374*, 88.
11. Zhang, S.; Awaja, F.; James, N.; McKenzie, D. R; Ruys, A. J. *Polym. Adv. Technol.* **2011**, *22*, 2496.
12. Awaja, F.; Zhang, S.; James, N.; McKenzie, D. R. *Plasma Proc. Polym.* **2010**, *7*, 1010.
13. Awaja, F.; Zhang, S; James, N; McKenzie, D. R. *Plasma Proc. Polym.* **2010**, *7*, 866.
14. Awaja, F; Gilbert, M.; Kelly, G.; Fox, B; Pigram, P. J. *Prog. Polym. Sci.* **2009**, *34*, 948.
15. Katzer, A.; Marquardt, H.; Westendorf, J.; Wening, J. V.; von Foerster, G. *Biomaterials* **2002**, *23*, 1749.
16. Mastronardi, L.; Ducati, A.; Ferrante, L. *Acta Neurochir.* **2006**, *148*, 307.
17. Wang, H.; Xu, M.; Zhang, W.; Kwok, D. T. K.; Jiang, J.; Wu, Z.; Chu, P. K. *Biomaterials* **2010**, *31*, 8181.
18. Ismail, F.; Rohanizadeh, R.; Atwa, S.; Mason, R.; Ruys, A.; Martin, P; Bendavid, A. *J. Mater. Sci. Mater. Med.* **2007**, *18*, 705.
19. Martin, J. Y.; Schwartz, Z; Hummert, T. W.; Schraub, D. M.; Simpson, J.; Lankford, J.; Dean, D. D.; Cochran, D. L.; Boyan, B. D. *J. Biomed. Mater. Res.* **1995**, *29*, 389.
20. Lee, S. J.; Choi, J. S.; Park, K. S.; Khang, G.; Lee, Y. M; Lee, H. B. *Biomaterials* **2004**, *25*, 4699.
21. Anselme, K. *Biomaterials* **2000**, *21*, 667.
22. Carisey, A; Ballestrem, C. *Eur. J. Cell Biol.* **2011**, *90*, 2–3, 157.
23. Ziegler, W. H.; Liddington, R. C.; Critchley, D. R. *Trends Cell Biol.* **2006**, *16*, 9, 453.
24. DeMali, K. A. *Trends Biochem. Sci.* **2004**, *29*, 11, 565.
25. Saunders, R. M.; Holt, M. R.; Jennings, L.; Sutton, D. H.; Barsukov, I. L.; Bobkov, A.; Liddington, R. C.; Adamson, E. A.; Dunn, G. A.; Critchley, D. R. *Eur. J. Cell Biol.* **2006**, *85*,6, 487.
26. Rochford, E. T. J.; Poulsson, A. H. C.; Salavarrieta, V. J.; Lezuo, P.; Richards, R. G.; Moriarty, T. F. *Colloids Surfaces B: Biointerfaces* **2014**, *113*, 213.
27. Rochford, E. T. J.; Jaekel, D. J.; Hickok, N. J.; Richards, R. G.; Moriarty, T. F.; Poulsson, A. H. C. Bacterial interactions with polyaryletheretherketone. In: PEEK Biomaterials Handbook; Kurtz, A., Ed.; Elsevier, **2012**; Chapter 8, p 93–117.
28. Poulsson, A. H. C.; Eglin, D.; Zeiter, S.; Camenisch, K.; Sprecher, C.; Agarwal, Y.; Nehrbass, D.; Wilson, J.; Richards, R. G. *Biomaterials* **2014**, *35*, 12, 3717.
29. Speranza, G.; Laidani, N. *Part I Diam. Rel. Mat.* **2004**, 13/3, 445.
30. Forsey, R.; Chaudhuri, J. *Biotechnol. Lett.* **2009**, *31*, 819.
31. Ramaker, D. E. *Rev. Sol. Stat. Mater. Sci.* **1991**, *17*, 211.
32. Mizokawa, Y.; Miysato, T.; Nakamura, S.; Geib, K. M.; Wilmsen, C. *J. Vac. Sci. Technol.* **1987**, *5*, 2809.
33. Ramaker, D. E. *J. Vac. Sci. Technol.* **1989**, *3*, 1614.